Journal of Applied Polymer Science

Voltage-induced wrinkling behavior of dielectric elastomer

Xuejing Liu,[1,2] Bo Li,[1,2] Hualing Chen,[1,2] Shuhai Jia,[1,2] Jinxiong Zhou[2,3]
[1]School of Mechanical Engineering, Xi'an Jiaotong University, Xi'an 710049, China
[2]State Key Laboratory for Strength and Vibration of Mechanical Structures, Xi'an Jiaotong University, Xi'an 710049, China
[3]School of Aerospace, Xi'an Jiaotong University, Xi'an 710049, China
Correspondence to: B. Li (E-mail: liboxjtu@mail.xjtu.edu.cn)

ABSTRACT: Wrinkles, with regular periodic patterns in soft dielectric membrane, are interesting, since they are induced electrically by applying a voltage. An experimental investigation is presented to study the wrinkling behavior of dielectric elastomer. Steady wrinkles, without the accompany of electrical breakdown were attained. According to the relationship between wrinkling and breakdown, the electromechanical behaviors of DE membrane can be divided into the following types: Type A: breakdown directly without wrinkles; Type B: wrinkle and immediate breakdown; Type C: form steady wrinkles within a voltage span. Three different electromechanical behaviors of DE membrane are classified in a phase chart. A theoretical analysis is presented and discussed, involving the effect of prestretch and configurations to predict the relationship between mechanical wrinkling and electrical breakdown. Wrinkles at on-demand location can be triggered. The results agree with the experiments. © 2015 Wiley Periodicals, Inc. J. Appl. Polym. Sci. **2016**, *133*, 43258.

KEYWORDS: dielectric properties; elastomers; functionalization of polymers; mechanical properties; theory and modeling

Received 18 July 2015; accepted 22 November 2015
DOI: 10.1002/app.43258

INTRODUCTION

Wrinkling is an ubiquitous phenomenon and can be observed in various occasions, for example, aging of human skins, dehydration of fruits, and cascade of a window curtain.[1,2] Wrinkles with regular spatial periodicity are useful in extensive applications, including metrology,[3,4] complex surface patterning,[5–7] 3-D mechanical fabrication,[8,9] smart adhesion,[10,11] and optical gratings.[12,13]

Wrinkles appear mostly in compliant materials. They are elastomers, gels, membranes, and biological tissues.[14] The nonlinearity in material elasticity enables these materials to wrinkle rather than buckle. Based on this principle, wrinkles can evolve into complex surface patterns during instability, i.e. creases, craters, folds, and ridges, when different soft layers are dedicatedly manipulated.[15–17] The mechanisms for wrinkling are different, and the performances of wrinkling have been investigated experimentally and theoretically for the past several decades. Within these researches, the majority of underlying activations are, but not limited to, externally applied mechanical stress, temperature change, variation in pH values,[18–20] while little research is focused on electrical activation.[17,21]

As a sub-category of electro-active polymer, dielectric elastomer (DE) is a soft active material that can produce large deformation under electrical stimuli.[22] Previously, wrinkling of elastic membrane was investigated in a film–substrate system, in which wrinkles were activated by a compressive mechanical stress.[23] In recent work, the surface crease-wrinkling transition is then induced by voltage when the film is bonded to a rigid substrate.[17] Both of the above wrinkling behaviors occur in a bilayer system, but report of the electrical wrinkling in a single layer DE film is still missing. Electrical activation advances short responding time, what's more, wrinkling of the single layer DE membrane also features lightness and simplicity in configuration, as a specific favorability in practical applications. Electrical activated wrinkling of DE membrane offers various potential applications, such as optical switch, tunable grating, on-demand fabrication, phononic crystal structure, and bio-mimetic engineering.[24–26] However, studies of wrinkling of single layer DE membrane are seldom carried out.[27,28] The main reason is attributed to the electrical breakdown failure that occurred immediately after wrinkling.[29] Wrinkles, stabilized with regular wave length and amplitude, exist only in particular loading conditions when the prestretch and applied voltage levels are specifically programmed.[27] But to our knowledge, the on-demand wrinkling and control strategy in DE membrane are still lack of investigation. The relationship between voltage-induced wrinkling and electromechanical breakdown also need further systematic research.

In the present article, we design a set of experiments to probe the wrinkling behavior of dielectric elastomer. The DE membrane is prestretched and clamped by a square-ring frame and

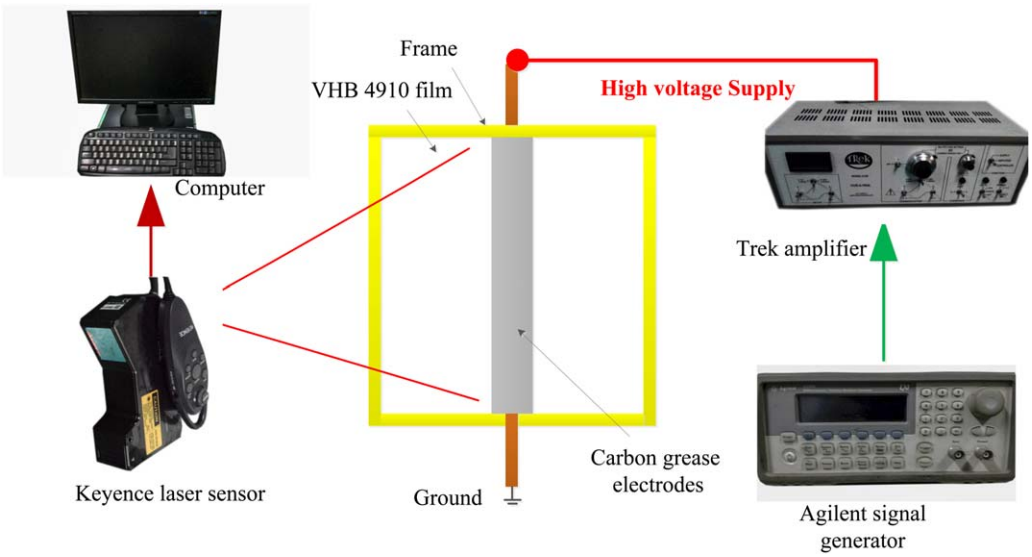

Figure 1. Experimental setup for measurement of the wrinkling in dielectric elastomer. [Color figure can be viewed in the online issue, which is available at wileyonlinelibrary.com.]

coated with strip-shape electrodes on both surfaces. The mechanical load is regulated by setting different prestretch levels on the membrane. In addition, different length–width ratios of electrode patterns on DE surfaces constitute different configurations, which can affect the wrinkling behavior. Through a series of experimental research, the condition for stable wrinkling without breakdown failure is determined and the nonlinear relationship between electromechanical breakdown and wrinkling is summarized and classified in a phase chart. Finally, a model is established to predict aforementioned wrinkling–breakdown (WB) relationships.

MATERIALS AND EXPERIMENTAL METHODS

The overall experimental setup is illustrated in Figure 1. Acrylic elastomer (VHB 4910 membrane, thickness of 1 mm, 3M Company) is selected as dielectric elastomer and used as received. The membrane is first stretched equal bi-axially in two in-plane directions. The prestretch of DE membrane is defined as the ratio of the length after mechanical stretch to the initial length, denoted by λ_p. And then the prestretch is maintained by sandwiching the membrane between two square-ring plastic frames. The inner edge length of the frame is fixed at $L = 80$ mm. Carbon grease No. 846 from MG Chemicals is used as compliant electrodes, which is brushed in the middle area of the membrane as an electro active area in a strip shape. The length of electrodes L_2 is equal to the inner edge length of frame L and the width of electrodes is denoted by L_A. Different length–width ratios can be achieved by adjusting L_A. A signal generator (No. 6811B, AgilentTM) and a voltage amplifier (No. 610E, Trek AmplifierTM) generate an incremental voltage Φ with a step of 20 V to the DE membrane until the electrical breakdown occurs. The morphology of the wrinkles is characterized by a two-dimensional laser displacement sensor (LK-G200-1, KeyenceTM) via measuring the out-of-plane deflection of the membrane.

The prestretches and length–width ratios ($\alpha = L/L_A$) are organized in combination in the experiments. We design five sets prestretches (2×2, 2.5×2.5, 3×3, 3.5×3.5, 4×4), three length–width ratios (5, 10, 20), and record two essential voltage values: wrinkling value and breakdown value, for each test. Meanwhile, the out-of-plane deformation is measured to provide evidence for voltage-induced wrinkling in DE membrane.

EXPERIMENTAL OBSERVATIONS

According to the experiments, we observed that when the voltage value was small, the membrane remained flat. When the voltage ramped up, exceeding a critical value, the membrane either suffered from electric breakdown directly, or formed wrinkles. Figure 2 shows that the activative area of the membrane exhibits wrinkles with regular waveforms without electrical breakdown.

Based on the chronological order of voltage-induced wrinkling and breakdown, the electromechanical behaviors of DE membrane are categorized into three types: Type A: direct electrical breakdown without wrinkles; Type B: wrinkles with immediate breakdown; Type C: steady wrinkles form within a voltage span. The experimental results are listed in Figure 3(a–e). Here λ-axis is defined as the actuation stretch in the length direction of DE membrane.

For weakly prestretched membranes, material breakdown directly before wrinkling. This is Type A behavior and the corresponding voltage values are listed in Figure 3(a,b). As we slightly enlarge the prestretch, the DE membrane undergoes a larger deformation and wrinkles at the critical voltage. The voltage is recorded and denoted as the wrinkle voltage. As the voltage continues to ramp up slightly (50–100 V), the membranes breakdown quickly. This is Type B behavior: wrinkling with a relatively low breakdown strength. Steady wrinkle is attainable in DE membrane with Type C behavior: the material can exhibit a large stretch, wrinkles are formed and maintained

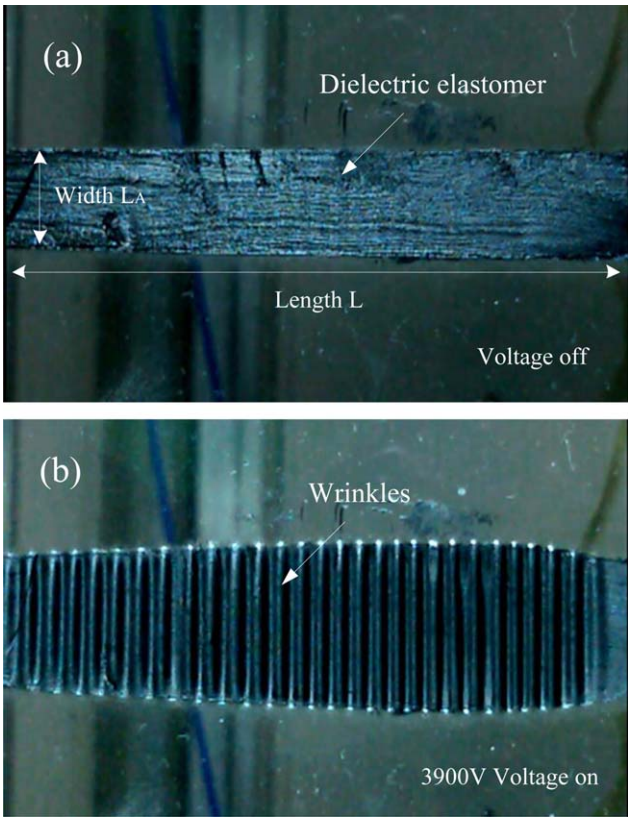

Figure 2. (a) Flat elastomer without voltage; (b) wrinkled elastomer with voltage on. [Color figure can be viewed in the online issue, which is available at wileyonlinelibrary.com.]

within a considerable voltage span (500–1000 V) after stable wrinkles spread over the membrane. Both prestretch λ_p and length–width ratio $\alpha = L/L_A$ affect the wrinkling behavior. For example, in Figure 3(b,c), the wrinkling behavior of DE membrane transits from Type A to Type B and to Type C successively.

The electromechanical behaviors of DE membrane are summarized according to different length–width ratios and prestretch levels in a phase chart, as plotted in Figure 4. When the prestretch levels are small, the membranes breakdown directly (Type A) at all three length–width ratios. As we increase the prestretch level to a medium value, the membranes wrinkle first and breakdown immediately (Type B) after the voltages further ramp up. Steady wrinkles (Type C) are formed and maintained by high prestretch levels and large length–width ratios. In following studies, we focus on the mechanisms of the above electromechanical behaviors.

MODELLING AND DISCUSSION

We explain the mechanism as follows. Under an increasing voltage, the mechanical stress in length direction decreases, and when it reduces to zero, the DE membrane suffers loss of tension and wrinkles will propagate along the length direction. Since the lateral expansion in length direction is constrained by the frame, the membrane deflects out-of-plane and forms wrinkles.

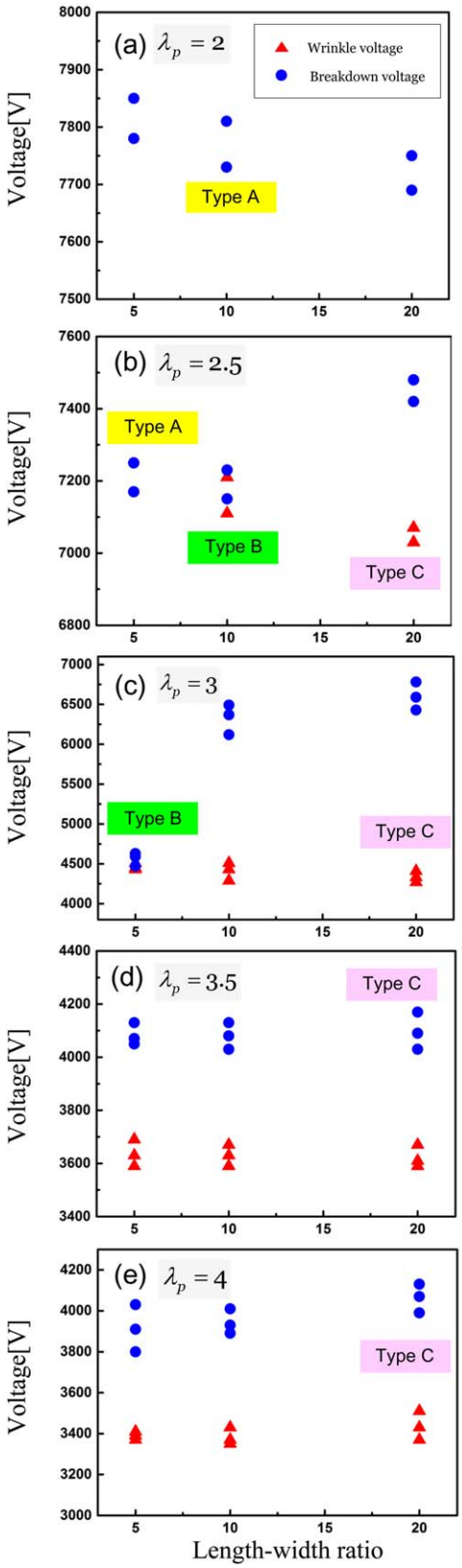

Figure 3. Three types of wrinkling process are classified with recorded voltages. [Color figure can be viewed in the online issue, which is available at wileyonlinelibrary.com.]

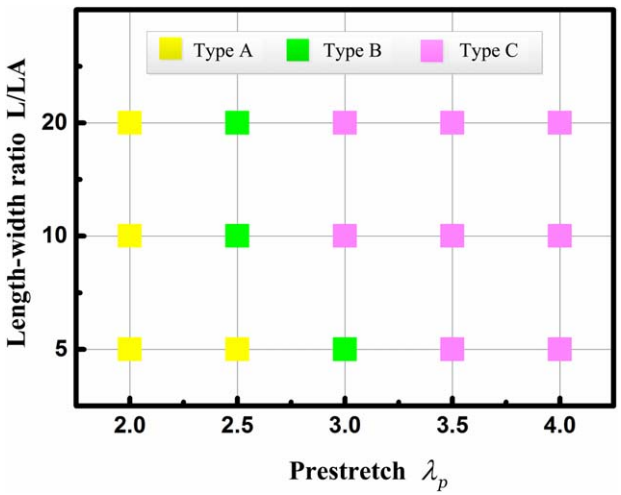

Figure 4. Phase chart of electromechanical behaviors of dielectric elastomer. [Color figure can be viewed in the online issue, which is available at wileyonlinelibrary.com.]

We then establish a physical model to characterize the complicated performance of wrinkling and breakdown. With reference to the experiments, in Figure 5, we define three states: reference state, pre-stretch state and voltage-actuation state. The initial DE membrane is of dimensions by $L_0 \times L_0 \times H$. Part A, the part of membrane that covered by compliant electrode and to be activated, is of initial length L_{A0}; while that of the two symmetric passive parts, namely part B, is L_{B0}, constituting $L_0 = L_{A0} + 2L_{B0}$. The membrane is then prestretched and fixed to a frame, so the length is enlarged by $\lambda_p$as $\lambda_p L_0 = L = \lambda_p L_{A0} + 2\lambda_p L_{B0}$. Subjected to an applied voltage Φ, the active part expands and passive part shrinks, generating the electromechanical strain; then the length is $\lambda_p L_0 = L = \lambda_A L_{A0} + 2\lambda_B L_{B0} = L_A + 2L_B$. The thickness of the active part is $\lambda_A^{-1}\lambda_p^{-1}H$. Here, we use λ to denote the level of deformation, either by mechanical stretch or by electrical voltage.

In order to simplify the calculation, several assumptions are made as follows: (a) the elastic stress of the passive parts is homogeneous; (b) regardless the stress concentration at four corners of the active part; (c) the deformation in direction 2

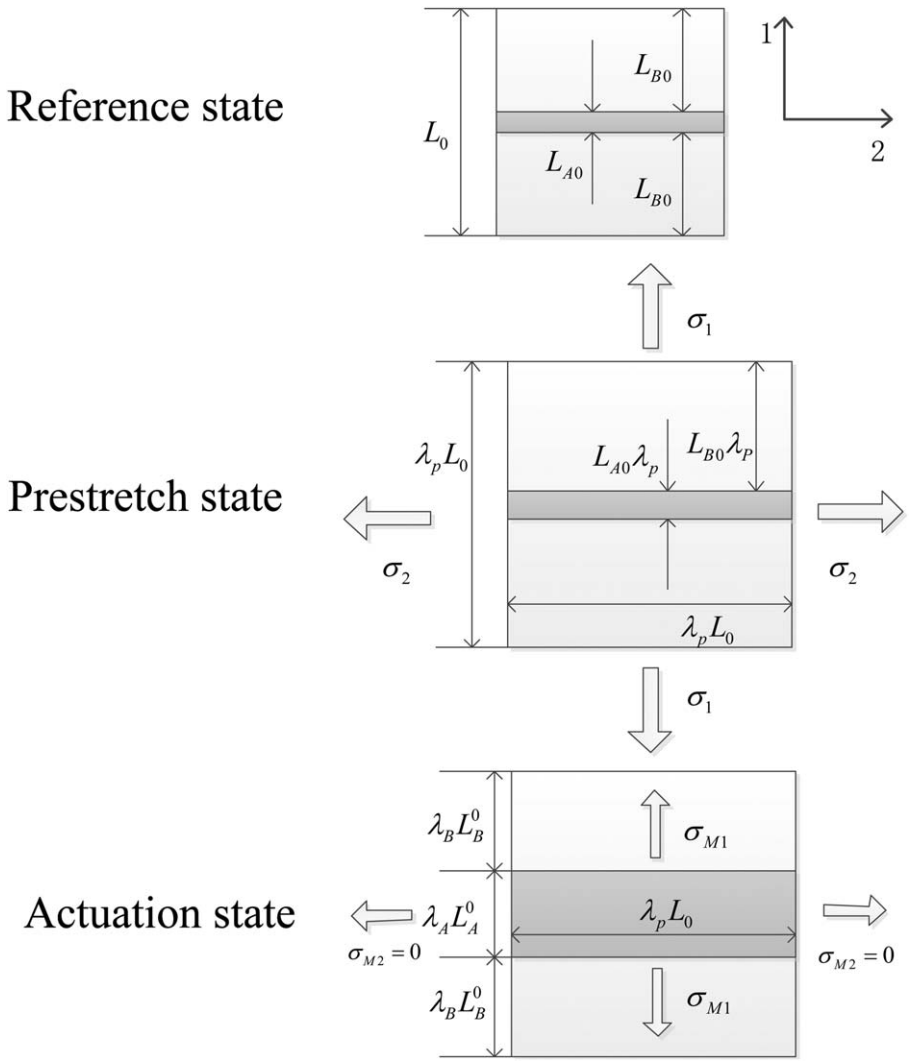

Figure 5. The DE membrane is stretched from (a) the initial state to (b) the prestretched state. With a voltage on, (c) the area with electrode expands, while the passive area shrinks.

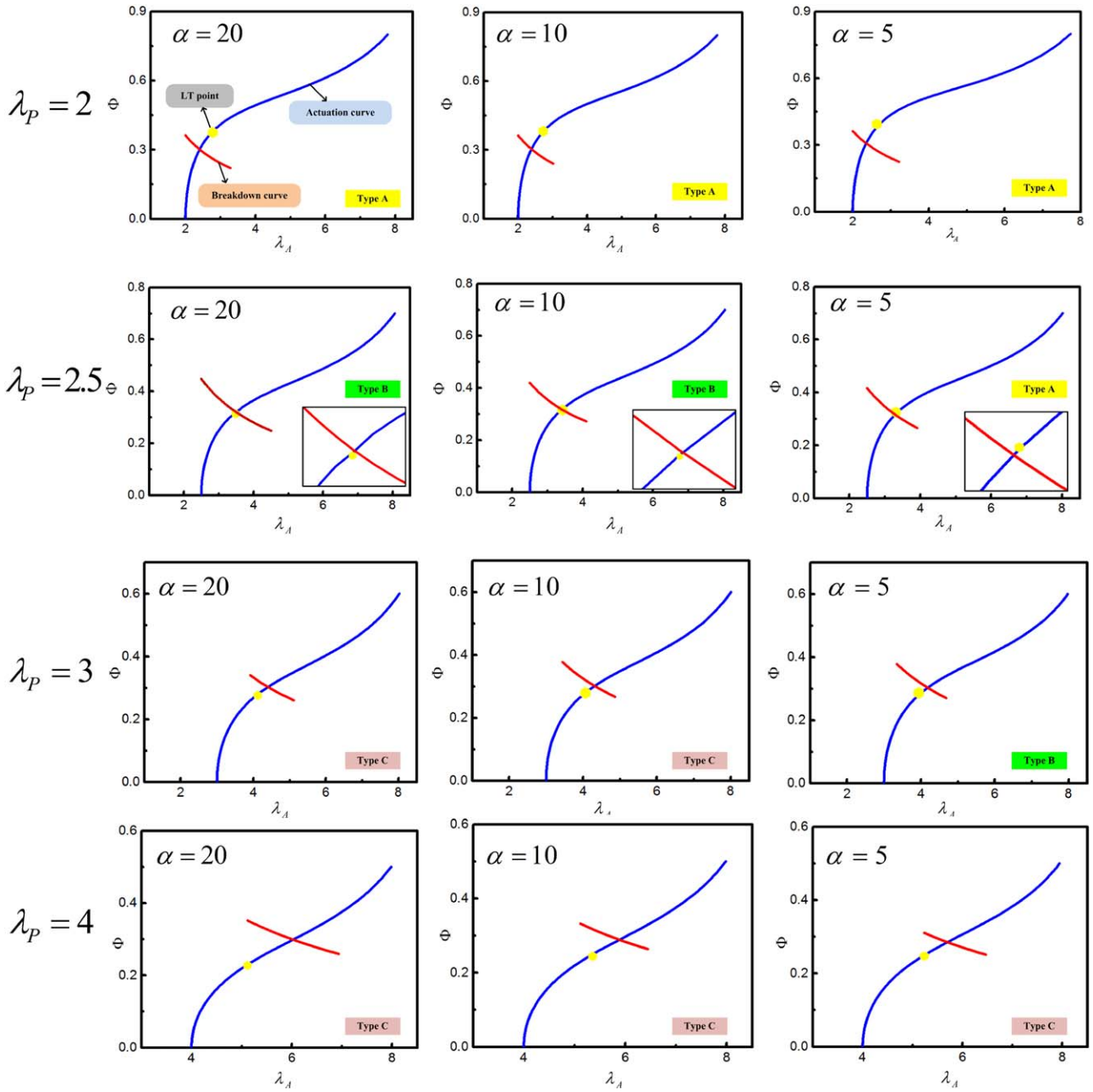

Figure 6. Modelling of three representative electromechanical behaviors of DE membrane under different prestretches and length–width ratios. [Color figure can be viewed in the online issue, which is available at wileyonlinelibrary.com.]

remains constant before wrinkling occurs, both active part and passive part, namely λ_p.

On the basis of the nonlinear field theory of dielectric elastomer, at the equilibrium state, the balance of stress is

$$\sigma_M + \sigma_E = \sigma_\lambda \tag{1}$$

where σ_M is the mechanical stress provided either by passive part of membrane or the rigid frame, σ_E is the electrostatic stress, σ_λ is the elastic stress because of the deformation.

First we consider the force balance in direction 1, denoted by 1 in the subscription. Because of the nonlinear hyper-elasticity, we employ the Gent strain energy function.

$$W_A = -\frac{J_m}{2}\mu \log\left(1 - \frac{\lambda_A^2 + \lambda_p{}^2 + \lambda_A^{-2}\lambda_p{}^{-2} - 3}{J_m}\right) \tag{2}$$

to characterize the deformation where μ is the shear modulus and J_{lim} is the extension limit. Therefore the elastic stress of part A in direction 1 with stretch λ_A takes the form as

$$\sigma_{\lambda 1} = \lambda_A \frac{\partial W_A}{\partial \lambda_A} \tag{3}$$

For the stress because of the electrostatic force, we express it via Maxwell stress as

$$\sigma_{E1} = \sigma_{E2} = \varepsilon E^2 = \varepsilon\left(\frac{\Phi}{H}\right)^2 \lambda_A^2 \lambda_p^2, \tag{4}$$

where ε is the permittivity.

For the mechanical stress provided by the passive parts, so the mechanical stress in direction 1 takes the form as

$$\sigma_{M1}=\lambda_B\frac{\partial W_B}{\partial \lambda_B} \tag{5}$$

Therefore, we have the expression on the equilibrium state of part A in direction 1

$$\lambda_B\frac{\partial W_B}{\partial \lambda_B}+\varepsilon\left(\frac{\Phi}{H}\right)^2\lambda_A^2\lambda_p^2=\lambda_A\frac{\partial W_A}{\partial \lambda_A} \tag{6}$$

with the energy function\

$$W_B=-\frac{J_m}{2}\mu\log\left(1-\frac{\lambda_B^2+\lambda_p{}^2+\lambda_B^{-2}\lambda_p{}^{-2}-3}{J_m}\right) \tag{7}$$

For part A in direction 2, as we increase the voltage, the membrane suffer loss of tension in direction 2 and form wrinkles, so at the critical point for wrinkling, the mechanical stressprovided by the frame vanishes $\sigma_{M2}=0$, and the expression is

$$\varepsilon\left(\frac{\Phi}{H}\right)^2\lambda_A^2\lambda_p^2=\lambda_p\frac{\partial W_A}{\partial \lambda_p} \tag{8}$$

As the result of fixed geometry in the frame, the total length is constant as $\lambda_p L_0=L=\lambda_A L_{A0}+2\lambda_B L_{B0}=L_A+2L_B$ thus we set $L/L_A=\alpha$, so the stretch in part B is

$$\lambda_B=\frac{\alpha\lambda_p-\lambda_A}{\alpha-1}. \tag{9}$$

Substituting Eq. (2), (4), (5), (7), (9) to (6), we obtain the constitutive equation for part A

$$\begin{aligned}&\mu\frac{\lambda_B^2-\lambda_B^{-2}\lambda_A{}^{-2}}{1-((\lambda_B^2+\lambda_p^2+\lambda_B^{-2}\lambda_p{}^{-2}-3)/J_m)}\\&+\varepsilon\left(\frac{\Phi}{H}\right)^2\lambda_A^2\lambda_p^2=\mu\frac{\lambda_A^2-\lambda_A^{-2}\lambda_p^{-2}}{1-((\lambda_A^2+\lambda_p^2+\lambda_A^{-2}\lambda_p^{-2}-3)/J_m)}\end{aligned} \tag{10}$$

Using the material parameters of $\mu=100\times10^3$ Pa, $J_m=100$, $\varepsilon=3.98\times10^{-11}$F/$m$, we are able to plot the voltage-stretch curves in Figure 6. Equation (9) and (10) shows the actuation performance is determined by the voltage Φ, the pre-stretch λ_p, and the length–width ratio α.

In the schematic voltage-stretch curves in Figure 6, the blue curves illustrate the equilibrium states for a clamped DE membrane under different prestretches and length–width ratios. The red curves represent the condition of electrical breakdown. The solid points represent that the membrane suffer loss of tension (LT) in direction 2. From the figures, it can be observed that when the prestretch is small, namely $\lambda_p=2$, the intersect point of voltage-stretch $\Phi(\lambda)$ curve and breakdown curve $\Phi_B(\lambda)$ happens before LT at all three length–width ratios that DE membrane suffers breakdown directly before the onset of wrinkles, following Type A process. When prestretch is slightly increased to $\lambda_p=2.5$–3, the instability is lightened, the intersect points of $\Phi(\lambda)$ and $\Phi_B(\lambda)$ curve will occur at larger stretches; in addition, as we increase the length–width ratios, the intersect of breakdown will also move backward, and LT tends to happen before the occurence of breakdown, realized the transition from Type A to Type B and Type C, these phenomena have the same trends with experimental observations in Figure 4. DE membrane with large prestretch, say $\lambda_p=4$, the LT occur first and steady wrinkles can be maintained in a relative large voltage span; from the figures it can be seen that as we increase the length–width ratios, the voltage span between wrinkling and breakdown increases. Comparing the twelve graphs in Figure 6 with the twelve points in the phase chart (Figure 4), it can be concluded that all the above theoretical predictions agree with experimental observations. Nevertheless, the voltage of wrinkling and breakdown cannot be predicted precisely, the deviation between experimental and theoretical results probably lies in the simplification in modelling with neglecting of viscoelasticity in DE membrane and transition area at the electrode boundary.

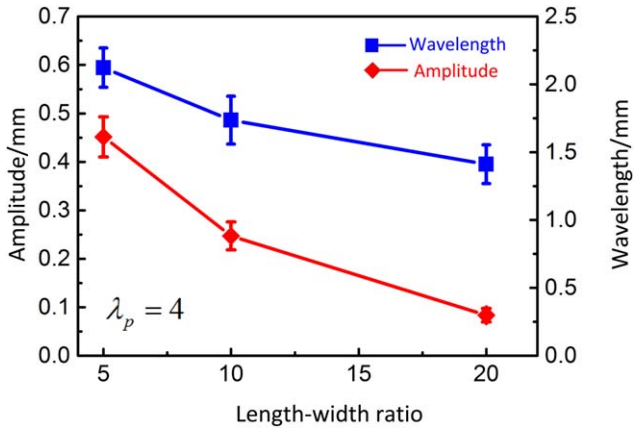

Figure 7. Amplitude and wave length in DE membrane versus length–width ratio. The prestretch is $\lambda_p=4$. [Color figure can be viewed in the online issue, which is available at wileyonlinelibrary.com.]

Uniform and steady wrinkles, whith are activated by voltage, are favorable in application. Here we characterize the wrinkled membrane with two essential parameters: wave length and amplitude. Wave length is defined as the distance between two adjacent wave crests and amplitude is defined as half of the distance between wave crest and trough. With reference to Figure 3(e), we prescribe $\lambda_p=4$ as an example of wrinkling case. By measuring the out-of-plane deflections, we are able to record the wave length/amplitude in different groups and handle the data in the form of error bars. The wave lengths and amplitudes of wrinkling morphologies, with respect to different prestretches are concluded in Figure 7. Both wave length and amplitude decreases with the increase of length–width ratio.

Wrinkling, induced by voltage, propagates on the surface of DE membrane. Here, we presented a detailed investigation for the membranes of prestretch $\lambda_p=4$ and length–width ratio of $L_2/D=5$. Figure 8 shows (a)-(c) the observation and (d)-(f) the characterization of the wrinkling morphology with the voltage of $\Phi=4990$, 5030, 5150 V respectively, for a complete process of wrinkle growth, from initialization to propagation. Under the voltage for the LT, the material deforms, thus the flat area and wrinkled area coexist in the membrane. As the voltage increases, the area for wrinkles expands at the expense of shrinkage of flat area, until the membrane is fully wrinkled.

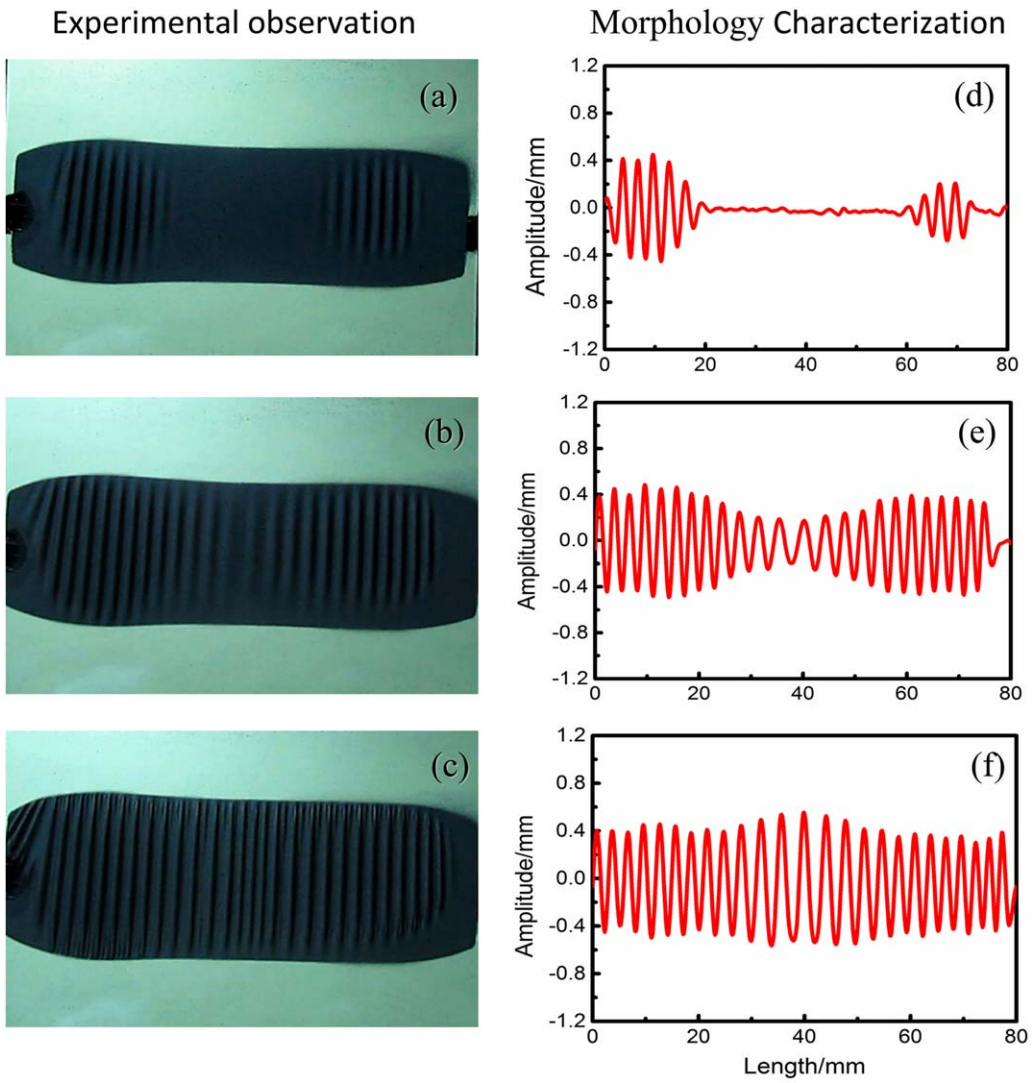

Figure 8. Comparison chart of experimental observation and morphology characterization of DE membrane. The prestretch is $\lambda_p = 4$ and the length–width ratio is $L_2/D = 5$. [Color figure can be viewed in the online issue, which is available at wileyonlinelibrary.com.]

Although the wave length and amplitude of wrinkled membrane cannot be predicted accurately now, the change law of the wave length and amplitude are acquired. In the future, more academic work should be conducted to simulate the morphology of wrinkled DE membrane.

This research may enrich the subject of soft material, adding new performance for wrinkled-based studies of coupled electromechanical fields. Wrinkle with on-demand location is now attainable. In the future, efforts could be spent to establish a reliable analytical model that can match wrinkling morphology of DE membrane. Thus wrinkle of pre-set periodicity will be realizable very soon.

CONCLUSIONS

In summary, we report the voltage-induced wrinkling deformation in single layer soft membrane. We design a set of experiments to investigate the voltage-induced wrinkling of soft dielectric membrane. Three different types of electromechanical behaviors are observed and classified in a phase chart. It is clear that steady wrinkles can be maintained by large prestretches and large length–width ratios. A model is established to predict the relationship between wrinkling and breakdown. The model can describe the whole set of experimental observations. The wrinkling morphology of DE membrane is characterized on its wave length and amplitude. Both the wave length and amplitude of wrinkles decrease with length–width ratios. Voltage-induced wrinkling of DE membranes may offer potential application in optical switch, on-demand fabrication, phononic crystal structure and bio-mimetic engineering in the future. The research provides new insights in the study of mechanics of soft active materials.

ACKNOWLEDGMENTS

This research was supported by the National Natural Science Foundation of China (Grant Nos. 11402184, 11472210 and 11321062), Shaanxi Province and China Postdoctoral Science Foundation

(Grant No. 2014M560761). B. L. acknowledges XJTU for the startup fund and international collaboration fund.

REFERENCES

1. Cerdaand Mahadevan, E. L. *Phys. Rev. Lett.* **2003**, *90*, 074302.
2. Schweikartand Fery, A. A. *Microchim. Acta* **2009**, *165*, 249.
3. Stafford, C. M.; Harrison, C.; Beers, K. L.; Karim, A.; Amis, E. J.; VanLandingham, M. R.; Kim, H. C.; Volksen, W.; Millerand, R. D.; Simonyi, E. E. *Nat. Mater.* **2004**, *3*, 545.
4. Chung, J. Y.; Nolteand, A. J.; Stafford, C. M. *Adv. Mater.* **2011**, *23*, 349.
5. Bowden, N.; Brittain, S.; Evans, A. G.; Hutchinsonand, J. W.; Whitesides, G. M. *Nature* **1998**, *393*, 146.
6. Cai, S.; Breid, D.; Crosby, A. J.; Suoand, Z.; Hutchinson, J. W. *J. Mech. Phys. Solids* **2011**, *59*, 1094.
7. Miquelard-Garnier, G.; Croll, A. B.; Davisand, C. S.; Crosby, A. J. *Soft Matter* **2010**, *6*, 5789.
8. Khang, D. Y.; Jiang, H.; Huangand, Y.; Rogers, J. A. *Science* **2006**, *311*, 208.
9. Chandraand, D.; Crosby, A. J. *Adv. Mater.* **2011**, *23*, 3441.
10. Chan, E. P.; Smith, E. J.; Haywardand, R. C.; Crosby, A. J. *Adv. Mater.-Deerfield Beach Then Weinheim.* **2008**, *20*, 711.
11. Davis, C. S.; Martina, D.; Creton, C.; Lindnerand, A.; Crosby, A. J. *Langmuir* **2012**, *28*, 14899.
12. Harrison, C.; Stafford, C. M.; Zhangand Karim, W. A. *Appl. Phys. Lett.* **2004**, *85*, 4016.
13. Yu, C.; O'Brien, K.; Zhang, Y. H.; Yuand Jiang, H. H. *Appl. Phys. Lett.* **2010**, *96*, 041111.
14. Genzerand Groenewold, J. J. *Soft Matter* **2006**, *2*, 310.
15. Cao, C.; Chan, H. F.; Zang, J.; Leongand, K.; Zhao, W. X. *Adv. Mater.* **2014**, *26*, 1763.
16. Wang, Q.; Zhangand Zhao, L. X. *Phys. Rev. Lett.* **2011**, *106*, 118301.
17. Wangand Zhao, Q. X. *Phys. Rev. E* **2013**, *88*, 042403.
18. Cote, L. J.; Kim, J.; Zhang, Z.; Sunand Huang, C. J. *Soft Matter* **2010**, *6*, 6096.
19. Park, J. Y.; Chae, H. Y.; Chung, C. H.; Sim, S. J.; Park, J.; Leeand, H. H.; Yoo, P. J. *Soft Matter* **2010**, *6*, 677.
20. Takei, A.; Brau, F.; Romanand Bico, B. J. *EPL (Europhys. Lett.)* **2011**, *96*, 64001.
21. Huang, R. *Appl. Phys. Lett.* **2005**, *87*, 151911.
22. Suo, Z. *Acta Mech. Solida Sin.* **2010**, *23*, 549.
23. Wangand Zhao, Q. X. *J. Appl. Mech.* **2014**, *81*, 051004.
24. Connand, A.; Rossiter, T. J. *Appl. Phys. Lett.* **2012**, *101*, 171906.
25. Palacios-Cuesta, M.; Cortajarena, A. L.; Garcíaand Rodríguez-Hernández, O. J. *Polymers* **2014**, *6*, 2845.
26. Wang, Y.; Zhou, J.; Sun, W.; Wuand Zhang, X. L. *Smart Mater. Struct.* **2014**, *23*, 095010.
27. Kollosche, M.; Zhu, J.; Suoand Kofod, Z. G. *Phys. Rev. E* **2012**, *85*, 051801.
28. Mao, G.; Huang, X.; Diab, M.; Li, T.; Quand Yang, S. W. *Soft Matter* **2015**, *11*, 6569.
29. Planteand, J.; Dubowsky, S. S. *Int. J. Solids Struct.* **2006**, *43*, 7727.